

Oxygen-deficient effect on charge ordering in spin- and charge-frustrated ferrite $\text{YFe}_2\text{O}_{4-\delta}$

Y. Horibe

Rutgers Center for Emergent Materials and Department of Physics & Astronomy, Rutgers University, Piscataway, New Jersey 08854, USA

K. Yoshii

Japan Atomic Energy Agency, Sayo, Hyogo 679-5148, Japan

N. Ikeda

Department of Physics, Okayama University, Okayama 700-8530, Japan

S. Mori*

Department of Materials Science, Osaka Prefecture University, Osaka 599-8531, Japan

(Received 8 June 2009; revised manuscript received 25 August 2009; published 22 September 2009)

The effects of oxygen deficiency on charge ordering were investigated by transmission electron microscopy at various deficiencies and temperatures of $\text{YFe}_2\text{O}_{4-\delta}$. We found that the detailed nature of the charge ordering structures is associated with changes in the superlattice reflections and diffuse scattering. They go from $(1/3\ 1/3\ 1/2)$ -type superlattice reflection to $(1/3\ 1/3\ l)$ -type straight-type diffuse scattering, then to zigzag-type diffuse scattering. With the oxygen deficiencies increased, the interchange correlation of Fe-O bilayers obviously decreases, yet the triple superperiodicity along $[110]^*$ remains unchanged. These findings on frustrated ferrites indicate the stability of in-plane threefold charge ordering and the importance of the interchange interaction between bilayers in the structural phase transitions.

DOI: [10.1103/PhysRevB.80.092104](https://doi.org/10.1103/PhysRevB.80.092104)

PACS number(s): 77.80.Bh, 77.80.Dj, 68.37.Lp, 77.84.-s

Mixed-valence triangular lattice compounds $R\text{Fe}_2\text{O}_{4-\delta}$ ($R=\text{Y}$, Ho, Er, Tm, Yb, and Lu) have been extensively studied because of their multiferroicity and charge ordering (CO) on geometrically frustrated lattices.¹⁻³ $R\text{Fe}_2\text{O}_{4-\delta}$ has a rhombohedral crystal structure with the space group $R\bar{3}m$.⁴ This structure is characterized by the alternative stacking of triangular-lattice layers with Fe-O bilayers and R-O layers, indicating two dimensionality [Fig. 1(a)]. Furthermore, the same amount of Fe^{2+} and Fe^{3+} ions coexist at the Fe sites in the charge ordering state since the Fe valence is equal to 2.5+ in the chemical formula. The spin and charge ordering on the geometrically frustrated lattice in this system is expected to result in intriguing physical phenomena and structural changes.^{1-3,5-11} Charge imbalance within bilayers of the CO state gives rise to ferroelectricity, which is regarded as multiferroic.^{12,13} This indicates a new mechanism for ferroelectricity from the degree of freedom of spins and charges. Changes in $\text{LuFe}_2\text{O}_{4-\delta}$ and $\text{YFe}_2\text{O}_{4-\delta}$ with the superlattice reflections (SRs) and diffuse scatterings (DSs) are related to complicated structural phase transitions from the distinct CO.^{2,3,8-10} These results indicate the presence of lattice response to the complex CO state.

Physical properties in $R\text{Fe}_2\text{O}_{4-\delta}$ are well known to be especially sensitive to oxygen deficiencies (ODs). The stoichiometric YFe_2O_4 exhibits some anomalies at ~ 250 K in both the electric resistivity and magnetic susceptibility on warming (at ~ 240 K on cooling), which is suggested to be related to the three-dimensional CO transition.^{14,15} It has been reported that the electric and magnetic properties change in $\text{YFe}_2\text{O}_{4-\delta}$ drastically with different ODs.¹⁴⁻¹⁶ For example, the electric resistivities exhibit about four orders of magnitude difference (from 10^{-4} to 10^{-7} Ω cm).¹⁴ This leads

to the evolution of large hysteresis, among the polycrystalline specimens sintered under the wide range of oxygen partial pressures. Neutron diffraction studies suggested that the stoichiometric YFe_2O_4 shows three-dimensional spin ordering below ~ 235 K on cooling.¹⁶ Spin correlations in the nonstoichiometric $\text{YFe}_2\text{O}_{4-\delta}$ remain two dimensional until ~ 80 K (at the lowest temperature in the measurements).¹⁶ These results clearly imply that the magnetic ground states are significantly different in the stoichiometric and nonsto-

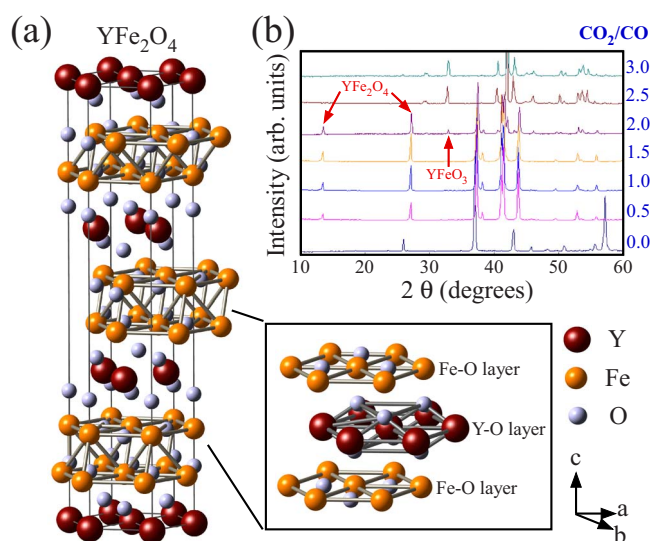


FIG. 1. (Color online) (a) Schematic of crystal structure of YFe_2O_4 . Part of a Y-O layer and Fe-O bilayers are also shown in the inset. (b) Powder x-ray diffraction patterns in the samples with different CO_2/CO mixture ratios.

ichiometric $\text{YFe}_2\text{O}_{4-\delta}$. Despite these studies, changes in the superstructures during the structural phase transitions have not been investigated systematically in the different ODs of $\text{YFe}_2\text{O}_{4-\delta}$. It is essential to clarify the effect of ODs on the structural changes in a proper understanding of anomalous physical properties due to COs.

In this Brief Report, we report that the structural phase transitions with respect to two-dimensional and three-dimensional COs are strongly associated with the level of ODs. With increased ODs the transition temperatures between different COs decrease monotonically, even though the CO superstructures with $(1/3\ 1/3\ 1/2)$ -type SRs, $(1/3\ 1/3\ l)$ -type straight-type DS, and zigzag-type DS remain unchanged. Our results clearly demonstrate the three-fold CO superstructure within Fe-O bilayer is surprisingly stable, on the other hand, interchange correlation between bilayers is sensitive to the OD compositions.

Polycrystalline specimens were used for the present study. The samples with different amounts of ODs (δ) were prepared by solid-state reaction method. They were sintered with 1210 °C at reduction atmosphere under careful control of the CO_2/CO gas ratio. It should be noted that oxygen partial pressure in the reduction atmosphere, which is significant to synthesize $\text{YFe}_2\text{O}_{4-\delta}$ phase, can be controlled by changing the CO_2/CO mixture ratio in the chemical equilibrium state. We used the gas-mixture ratio to identify samples with the different deficiencies, as reported previously,¹⁵ since absolute δ values were not measured in the present work. Crystallographic information was obtained from powder x-ray diffraction using the Fe target at room temperature. The specimens for the transmission electron microscopy (TEM) experiments were prepared by crushing in order to prevent additional defects by Ar-ion milling technique. The observation was carried out with the JEOL-2010 TEM equipped with liquid-nitrogen cooling specimen holder and heating specimen holder. The structural changes in $\text{YFe}_2\text{O}_{4-\delta}$ with various δ were investigated by obtaining both electron-diffraction (ED) patterns and real-space images related to the CO structure. Note that the indexes in the ED patterns are based on the rhombohedral space group of $R\bar{3}m$ (with hexagonal notation) in the same manner as follows.

The powder x-ray diffraction patterns in the samples with different CO_2/CO mixture ratios [Fig. 1(b)] clearly show that there exists $\text{YFe}_2\text{O}_{4-\delta}$ as a stable phase in the particular range of oxygen partial pressure in the reduction atmosphere, and the δ values in $\text{YFe}_2\text{O}_{4-\delta}$ can be continuously controlled by changing the oxygen partial pressure (i.e., by changing the CO_2/CO mixture ratio). The peaks at $2\theta = \sim 13.5^\circ$ and $\sim 27.1^\circ$ ($\sim 32.8^\circ$) in the profiles are characterized by the presence of the $\text{YFe}_2\text{O}_{4-\delta}$ (YFeO_3) phase. The samples with the gas mixture ratio of 0.5, 1.0, and 1.5 exhibit the single phase of $\text{YFe}_2\text{O}_{4-\delta}$, while that of 2.0 corresponds to the coexistence of $\text{YFe}_2\text{O}_{4-\delta}$ and YFeO_3 phases. The single YFeO_3 phase, in which the Fe valence is equal to 3+, is stabilized as the gas-mixture ratio increased. The mixture of Y_2O_3 and Fe (metal) can be found in the case of the ratio of 0.0, meaning pure CO gas. Three single phase $\text{YFe}_2\text{O}_{4-\delta}$ samples with the mixture ratio of 0.5 (R0.5), 1.0 (R1.0), and 1.5 (R1.5) are chosen for further experiments. According to the oxygen par-

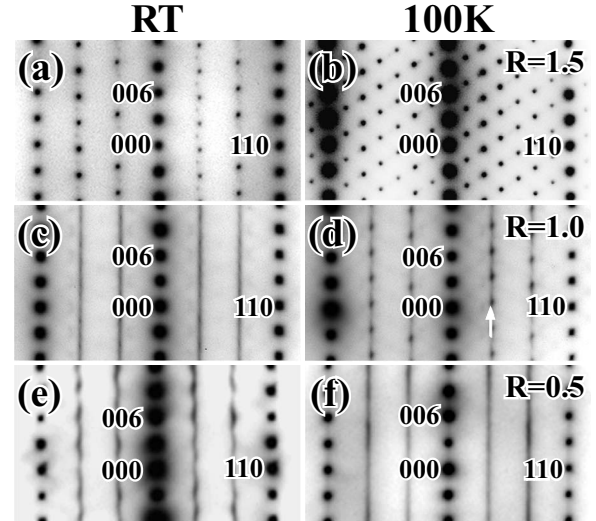


FIG. 2. Electron-diffraction patterns in the samples sintered under the different CO_2/CO gas mixture ratio of 1.5 [(a) and (b)], 1.0 [(c) and (d)], and 0.5 [(e) and (f)], respectively. The diffraction patterns are obtained at RT for (a), (c), and (e), and at ~ 100 K for (b), (d), and (f), respectively. The electron-beam incidence is parallel to the $[1\bar{1}0]$ direction.

tial pressure expected, the R1.5 (R0.5) sample should have the least (most) ODs, and R1.0 sample corresponds to somewhere in the middle. It is worth mentioning that our careful analysis of powder x-ray diffraction patterns indicate that the c axis of the unit cell ($c = \sim 24.7$ Å) barely changes by δ in our experimental uncertainties. We measured the temperature dependence of the electric resistivity on warming and confirmed that the results are consistent with the previous report.^{15,17} The temperature dependence of the magnetic susceptibility in R1.5 was also measured and is basically the same as that for $x=0.00$.¹⁶

In order to investigate the dependence of the ODs on the CO, we thoroughly examined ED patterns in the samples with various δ . We found that the CO structure is best demonstrated by the presence of the SRs or DSs in the ED patterns with the electron incidence parallel to the $[1\bar{1}0]$ direction. Figure 2 shows the ED patterns with the electron-beam incident parallel to the $[1\bar{1}0]$ direction in R1.5 [(a) and (b)], R1.0 [(c) and (d)], and R0.5 [(e) and (f)] samples, respectively. The diffraction patterns are obtained at RT for (a), (c), and (e), and at ~ 100 K for (b), (d), and (f), respectively. In the ED patterns shown in Figs. 2(a) and 2(b), there exist $(1/3\ 1/3\ 1/2)$ -type SRs with the weak DS (and $(1/3\ 1/3\ 3/2)$ spots due to twinning) at RT and $(1/7\ 1/7\ 9/7)$ -type SRs at 100 K. On the other hand, as in Figs. 2(c) and 2(d), the straight DS going through $(1/3\ 1/3\ 0)$ -type positions, without intensity maxima, can be seen at RT in the R1.0 sample, while the $(1/3\ 1/3\ 1/2)$ -type SRs appear at 100 K with the DS. In the case of the R0.5 sample, which contains the most ODs, the zigzag-type DS at RT turns into the straight DS at 100 K. On warming from RT the SRs in the R1.5 become the coexistence of the SRs and DS and finally become only DS at ~ 500 K (not shown here). These results imply that the changes in the SRs

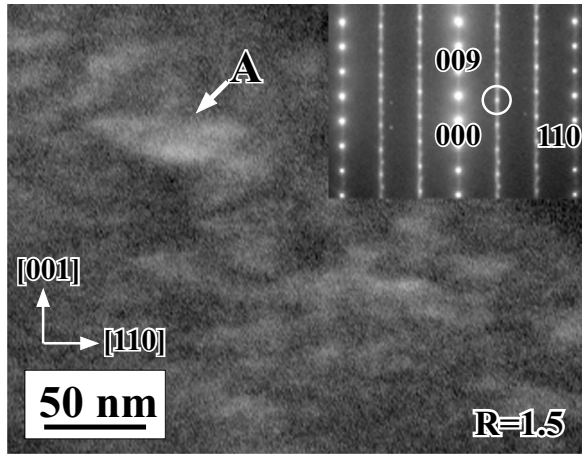


FIG. 3. High-resolution dark-field image at room temperature in the $\text{CO}_2/\text{CO}=1.5$ sample. (Inset) the electron-diffraction pattern corresponding to the image. Note that the electron-beam incidence is parallel to the $[1\bar{1}0]$ direction. The $(1/3\ 1/3\ 5/2)$ superlattice spot used for the dark-field imaging is framed by a circle.

and DSs obviously exhibit the dependence of the ODs, and that the transition temperatures among the COs, surprisingly, decrease significantly in the intensively wide range of the ODs. It should be emphasized that the ED pattern in the ferroelectric phase of LuFe_2O_4 shows the similar pattern to Fig. 2(a), without the weak DS.² It is worth mentioning that in typical CO materials such as manganites the superperiodicity of the CO should be proportional to the doped carrier concentration, which can be modified by ODs.¹⁸ Therefore it is suggested that the threefold CO superstructures within bilayers turn out to be robust in the different δ , however, the interchange interaction between bilayers appear to be more sensitive to the ODs. Since the formation of the CO structures are closely related to the compensation of the geometrical frustration, these results suggest one of the characteristic features in the frustrated CO systems. It should be noted that the presence of $(1/3\ 1/3\ 1/2)$ SRs in our experimental results is inconsistent with the CO model proposed in the previous TEM study.^{19,20} On the other hand, our experimental results are consistent with the model proposed on the x-ray diffraction experiments by Angst *et al.*²¹

We carefully examined real-space images of the CO in the R1.5 sample at room temperature. Figure 3 is the high-magnification dark-field image taken by using the $(1/3\ 1/3\ 5/2)$ SRs framed by a circle in the inset of the ED pattern. CO domains, about ~ 40 nm in width \times ~ 25 nm in thickness, can be clearly seen, as shown by the arrow A. The most striking feature is the asymmetric shape of the CO domain, i.e., platelike form. This indicates that the correlation length of the CO parallel to the c axis (~ 25 nm, about 10 unit cells/30 bilayers) is shorter than that within bilayers (~ 40 nm, about 120 unit cells).

We clearly demonstrated the relationship between the ODs and the CO superstructures. Here we discuss a possible scenario for the evolution of the CO in $\text{YFe}_2\text{O}_{4-\delta}$ during the transitions on the basis of the present experimental results. It is well known that in layered lanthanoid ionic crystals, ionic

bonding between lanthanoid and oxygen ions is significant and, in general, very stable. The oxygen deficiencies are, therefore, readily introduced not to the lanthanoid-oxygen layers but to the other layers, i.e., the Fe-O bilayers in $\text{YFe}_2\text{O}_{4-\delta}$. Recent theoretical analyses pointed out that because of the compensation of the frustration the threefold CO superstructure can be more stable than the other COs such as fourfold CO.²² This is consistent with our experimental results. In fact, the threefold CO superstructure is very robust throughout the introduction of the ODs. As for the origin of the interchange interaction between bilayers, there will be two possibilities. One is the electrostatic interaction, and the other is the presence of the local lattice modulation coupled with distortions of the unit cell. The recent convergent beam electron-diffraction study indicated that in $\text{LuFe}_2\text{O}_{4-\delta}$ a crystal structure with the zigzag-type DS shows the point group of $3m$ at RT.¹⁹ This suggests that the structure can remain the three-fold rotational symmetry in the two-dimensional CO state, within the experimental conditions of the electron-beam probe size and radiation intensity. These imply that the rhombohedral cell is undistorted from the high-symmetric one (non-CO structures), and the two-dimensional CO structures, therefore, cannot have the interchange interaction through the lattice distortions. From the analogies, the interchange interaction between the Fe-O bilayers in $\text{YFe}_2\text{O}_{4-\delta}$ can be achieved by the intermediary of electrostatic interplay, across the Y-O layers. From the comparison of x-ray diffraction experiments and theoretical analysis in $\text{LuFe}_2\text{O}_{4-\delta}$,³ the straight-type and zigzag-type DSs can be explained if the interchange interaction of charges between the neighboring bilayers is taken into account. In the CO state the ODs are thought to compensate the charge imbalance between upper and lower Fe-O layers within a bilayer. In other words, the ODs can result in the weak interchange interaction between bilayers via weak electrostatic interplay. In fact the polarization within bilayer, which is related to the charge imbalance, is suppressed by the presence of ODs from the theoretical analysis.²²

The appearance of commensurate three-dimensional threefold CO characterized by $(1/3\ 1/3\ 1/2)$ -type SR cannot be well stabilized by the electrostatic-interaction mechanism. Local lattice modulation accompanied by unit-cell distortions can be the mechanism to stabilize the three-dimensional CO, where the local structure can differ from the rhombohedral *averaged* structure. The CO-lattice coupling can, therefore, provide the interchange interaction. This type of local lattice modulation serves as the additional compensation for the frustration in the CO state. In fact, $1q$ -type lattice modulation in the nanosized CO domains with about 40 nm in size, similar in size to the present work, has been found by the high-resolution TEM observations.²³ From our experimental results as well as the theoretical analysis,²² the threefold CO superstructure is robust over the introduction of the ODs, implying that amplitude of the charge modulation may become small. This may result in the reduction in the corresponding lattice distortion, therefore, the interchange interaction. The lattice-coupled interchange interaction can be a possible origin for the two-dimensional (or, nearly three dimensional, to be precise) CO states. The recent energy-

filtered TEM observations show the presence of the CO domains at about 295 K in $\text{YbFe}_2\text{O}_{4-\delta}$ with ~ 5 nm in width $\times \sim 1-2$ nm in thickness when zigzag-type DS appears.²⁴ We believe that the presence of the local lattice modulation and its evolution depending on the ODs as well as the temperatures should play an essential role in the structural phase transitions in this system. Further studies will be needed to figure out the details.

In summary, the successive structural phase transitions related to the CO are accompanied by the changes from zigzag-type DS to $(1/3\ 1/3\ l)$ -type straight DS, and then to $(1/3\ 1/3\ 1/2)$ -type SR with varying temperature and ODs. In addition, there are changes to $(1/7\ 1/7\ 9/7)$ -type SR in the stoichiometric samples, which is significantly different from the others. As the ODs increase, interchange interaction be-

tween bilayers obviously decreases, yet the in-plane threefold CO superstructure seems to be robust. These findings indicate the importance of the stability of in-plane threefold CO, the interchange interaction between bilayers, and the local lattice modulation in the phase transitions of this system.

The authors would like to thank S. W. Fackler, S. Ishihara, W. Wu, V. Kiryukhin, and S.-W. Cheong for their valuable discussions. This work was partially supported by a Grant-in-Aid for Scientific Research on Priority Areas "Novel States of Matter Induced by Frustration" (Grant No. 19052002) and KIBAN (B) (Grant No. 20340078) from the Ministry of Education, Culture, Sports, Science, and Technology in Japan.

*Corresponding author; mori@mtr.osakafu-u.ac.jp

- ¹N. Ikeda, H. Kito, J. Akimitsu, K. Kohn, and K. Siratori, *J. Phys. Soc. Jpn.* **63**, 4556 (1994).
- ²Y. Yamada, S. Nohdo, and N. Ikeda, *J. Phys. Soc. Jpn.* **66**, 3733 (1997).
- ³Y. Yamada, K. Kitsuda, S. Nohdo, and N. Ikeda, *Phys. Rev. B* **62**, 12167 (2000).
- ⁴K. Kato, I. Kawada, N. Kimizuka, and T. Katsura, *Z. Kristallogr.* **143**, 314 (1975).
- ⁵N. Ikeda, K. Kohn, H. Kito, J. Akimitsu, and K. Shiratori, *J. Phys. Soc. Jpn.* **64**, 1371 (1995).
- ⁶N. Ikeda, K. Odaka, E. Takahashi, K. Kohn, and K. Shiratori, *Ferroelectrics* **190**, 191 (1997).
- ⁷N. Ikeda, K. Kohn, N. Myouga, E. Takahashi, H. Kitoh, and S. Takekawa, *J. Phys. Soc. Jpn.* **69**, 1526 (2000).
- ⁸N. Ikeda, R. Mori, K. Kohn, M. Mizumaki, and T. Akao, *Ferroelectrics* **272**, 309 (2002).
- ⁹N. Ikeda, R. Mori, S. Mori, and K. Kohn, *Ferroelectrics* **286**, 175 (2003).
- ¹⁰Y. Horibe, K. Kishimoto, S. Mori, and N. Ikeda, *J. Korean Phys. Soc.* **46**, 192 (2005).
- ¹¹A. Nagano, M. Naka, N. Nasu, and S. Ishihara, *Phys. Rev. Lett.* **99**, 217202 (2007).
- ¹²N. Ikeda, H. Ohsumi, K. Ohwada, K. Ishii, T. Inami, K. Kakurai, Y. Murakami, K. Yoshii, S. Mori, Y. Horibe, and H. Kito, *Nature (London)* **436**, 1136 (2005).
- ¹³S.-W. Cheong and M. Mostovoy, *Nature Mater.* **6**, 13 (2007).
- ¹⁴M. Inazumi, Y. Nakagawa, M. Tanaka, N. Kimizuka, and K. Shiratori, *J. Phys. Soc. Jpn.* **50**, 438 (1981).
- ¹⁵M. Tanaka, J. Akimitsu, Y. Inada, N. Kimizuka, I. Shindo, and K. Siratori, *Solid State Commun.* **44**, 687 (1982).
- ¹⁶S. Funahashi, J. Akimitsu, K. Siratori, N. Kimizuka, M. Tanaka, and H. Fujishita, *J. Phys. Soc. Jpn.* **53**, 2688 (1984).
- ¹⁷The temperature dependences of electric resistivities of R1.5, R1.0, and R0.5 are similar to those of $\text{CO}_2/\text{H}_2=2.5$, 1.5, and 1.0, respectively, in the previous report. Note that the oxygen partial pressures estimated from gas equilibrium constants in $\text{CO}_2/\text{CO}=1.5$, 1.0, and 0.5 are close to those estimated in $\text{CO}_2/\text{H}_2=2.5$, 1.5, and 1.0, respectively, at the thermal equilibrium states.
- ¹⁸C. H. Chen, S.-W. Cheong, and H. Y. Hwang, *J. Appl. Phys.* **81**, 4326 (1997).
- ¹⁹Y. Zhang, H. X. Yang, Y. Q. Guo, C. Ma, H. F. Tian, J. L. Luo, and J. Q. Li, *Phys. Rev. B* **76**, 184105 (2007).
- ²⁰Y. Zhang, H. X. Yang, C. Ma, H. F. Tian, and J. Q. Li, *Phys. Rev. Lett.* **98**, 247602 (2007).
- ²¹M. Angst, R. P. Hermann, A. D. Christianson, M. D. Lumsden, C. Lee, M.-H. Whangbo, J.-W. Kim, P. J. Ryan, S. E. Nagler, W. Tian, R. Jin, B. C. Sales, and D. Mandrus, *Phys. Rev. Lett.* **101**, 227601 (2008).
- ²²M. Naka, A. Nagano, and S. Ishihara, *Phys. Rev. B* **77**, 224441 (2008).
- ²³Y. Horibe, K. Kishimoto, S. Mori, and N. Ikeda, *J. Electron Microsc.* **54**, i87 (2005).
- ²⁴Y. Murakami, N. Abe, T. Arima, and D. Shindo, *Phys. Rev. B* **76**, 024109 (2007).